THE INSTITUTE OF PAPER CHEMISTRY, APPLETON, WISCONSIN

IPC TECHNICAL PAPER SERIES
NUMBER 70

LIMITING FLUX IN ULTRAFILTRATION OF MACROMOLECULAR SOLUTIONS

DANIEL R. TRETTIN AND MAHENDRA R. DOSHI

DECEMBER, 1978

Limiting Flux in Ultrafiltration of Macromolecular Solutions

Daniel R. Trettin

and

Mahendra R. Doshi

The Institute of Paper Chemistry
Appleton, Wisconsin 54911

The mass transfer equation describing the process of gel polarized ultrafiltration is solved using an integral method. The agreement between the closed form integral method solution and the exact numerical solution is excellent while the widely used film theory deviates considerably.

This paper has been submitted for publication in AIChE Journal.

SCOPE

Membrane ultrafiltration has gained increasing recognition over the past decade as a simple and convenient process for concentration, purification and separation of moderate to high molecular weight solutes from solutions. The main advantage is that ultrafiltration does not involve a phase change or interphase mass transfer. Basically, ultrafiltration involves the pressure-activated separation of chemical constituents which have different permeability through a membrane. As a pressurized solution flows past a selective membrane, solvent permeates through the membrane while rejected solute accumulates in the vicinity of the membrane. In order for the criterion of steady state mass transfer to be satisfied, the net rate of convective transport toward and parallel to the membrane surface must equal the rate of transport by diffusion away from the membrane surface. The net result is a layer of solution adjacent to the membrane surface of substantially greater solute concentration than that of the bulk solution within the channel.

The phenomenon of concentration polarization always operates to reduce the efficiency of the ultrafiltration process. It does so by decreasing the effective pressure gradient (by increasing osmotic backpressure at the membrane surface) and, when solute concentrations become large enough, by forming a gelatinous matrix structure upon the membrane surface. This "gel" layer offers an additional hydraulic resistance to solvent flow. When a laminar flow ultrafiltration system is operated in the "gel polarized" region, permeate flux rates are governed primarily by the transport mechanisms of forced convection and molecular diffusion. Pressure dependence is secondary — increase in pressure merely increases gel thickness with little effect on permeate flux. Objective of this paper is to develop a reliable closed form relationship for the limiting flux due to gel polarization.

CONCLUSIONS AND SIGNIFICANCE

The agreement between the closed form integral method solution and the more exact numerical solution, for the case of constant diffusion coefficient, is excellent, deviations being less than 1 percent. However, the widely used film theory underpredicts flux by 20 and 30 percent for $\underline{F}_g$ = 15 and 50, respectively, where $\underline{F}_g$ is the ratio of the gel concentration to the feed concentration.

In the case of concentration dependent diffusion coefficient, the integral method is satisfactory. Film theory results still deviate from the exact solution though not as much as in the case of constant diffusion coefficient.

On the basis of film theory, the plot of permeate flux against feed concentration on a semilog graph should yield a straight line. This line when extrapolated to zero flux gives the gel concentration. In view of the significant deviations between film theory results and exact solution, such an extrapolation is not valid and may underpredict gel concentration. We recommend that either experimental data should be taken over a wider range of feed concentration so that extrapolation could be reliable, or more exact theory should be used to determine gel concentration.

PREVIOUS DEVELOPMENTS

A quantitative prediction of solvent flux requires an analysis of the basic transport mechanisms which take place within the ultrafiltration system. Currently, the most widely accepted model is that advanced by Michaels (1968) using film theory principles. The film theory model is formulated on the assumption that axial convection in the mass equation may be accounted for in an indirect way. Constant fluid properties are assumed, and the model when applied to the gel-polarized region assumes wall concentration to be constant and equal to gel concentration of the solute material. Therefore, the mass balance equation reduces to:

$$\underline{v}\,\frac{\partial \underline{c}}{\partial \underline{y}} = \underline{D}\,\frac{\partial^2 \underline{c}}{\partial \underline{y}^2} \tag{1}$$

where the boundary conditions are

$$\text{at } \underline{y} = 0 \text{ (membrane surface)}, \ \underline{c} = \underline{c}_g \tag{2a}$$

and when solute rejection at the membrane surface is complete,

$$-\left|\underline{v}_w\right| \underline{c}_g = \underline{D}_g \left.\frac{\partial \underline{c}}{\partial \underline{y}}\right|_{\underline{y}=0} \tag{2b}$$

$$\text{at } \underline{y} \geq \delta(\underline{x}), \ \underline{c} = \underline{c}_B, \tag{2c}$$

where $\delta(\underline{x})$ equals the mass transfer boundary layer thickness.

Upon integration and substitution of the boundary conditions one gets

$$\left|\underline{v}_w\right| = \frac{\underline{D}}{\delta(\underline{x})} \ln\left[\frac{\underline{c}_g}{\underline{c}_B}\right] \tag{3}$$

For small values of $\left|\underline{v}_w\right|$, $\underline{D}/\delta(\underline{x})$ may be defined as the mass transfer coefficient, $\underline{k}$. The value of $\underline{k}$ is characteristically calculated by solving the solute balance equation where transverse convection has been neglected:

$$\underline{u}\,\frac{\partial \underline{c}}{\partial \underline{x}} = D\,\frac{\partial^2 \underline{c}}{\partial \underline{y}^2} \tag{4}$$

for either constant wall concentration or constant wall flux boundary condition. The method of solution is analogous to the corresponding Leveque heat transfer solution. Assuming a linear axial velocity profile, the results for a parallel plate system may be given as

$$\underline{k} = \underline{A}\left(\frac{\underline{D}^2\underline{a}}{3\underline{x}}\right)^{1/3} \tag{5}$$

where

$\underline{A}$ = 0.776 (for constant wall concentration)

$\underline{A}$ = 0.942 (for constant wall flux)

and $\underline{a} = 3\,\langle \underline{u} \rangle / \underline{h}$

In summary, it can be seen that the film theory analysis is a patching method by which axial dependence, which appears explicitly through the term, $\underline{u}\,\partial \underline{c}/\partial \underline{x}$, is replaced by one which arises implicitly through the boundary layer thickness $\delta(\underline{x})$.

One of the first extensive studies on ultrafiltration using the film theory was published by Blatt, et al. (1970). These investigators used natural macromolecular solutions such as casein, albumin and plasma, and their studies confirmed the existence of the pressure-independent gel-polarized region. Their data displayed trends in system performance as predicted by film theory, however, quantitative agreement was not good. The main drawbacks of their experimental procedure were undeveloped flow at the entrance, pulsating flows due to the use of peristaltic pump and inconsistencies and ambiguities in reported system design (Blatt, 1978). It is recommended that their data be used only as a secondary source of information.

Goldsmith (1971) did some experiments using Dextran and Carbowax solutions. His work pointed out the importance of considering the osmotic pressure effect at the membrane surface. His data were analyzed by solving two simultaneous equations, one derived from the film theory,

$$|\underline{v}_{\underline{w}}| = \underline{k} \ln \left[\frac{\underline{c}_{\underline{w}} - \underline{c}_{\underline{P}}}{\underline{c}_{\underline{B}} - \underline{c}_{\underline{P}}} \right] \tag{6a}$$

and the other was a phenomenological law, relating permeate flux to the effective driving force,

$$|\underline{v}_{\underline{w}}| = \overline{\underline{A}} \, (\Delta \underline{p} - \Delta \pi) \tag{6b}$$

Goldsmith was primarily interested in the study of solute rejection phenomenon. Both parallel plate and stirred cell systems were studied in laminar and turbulent flow. Since only partially-developed flow was attained in the test unit, the mass transfer coefficient expression of

$$\frac{\underline{k}\underline{d}}{\underline{D}} = 0.664 \left(\underline{Re} \cdot \frac{\underline{d}}{\underline{\ell}} \right)^{1/2} \underline{Sc}^{1/3} \tag{6c}$$

was used. Because of the fact that reported data were mainly in the pre-gel region and the membranes used were very permeable to solute molecules, Goldsmith's data are not relevant to the present work.

Kozinski and Lightfoot (1972) developed a theoretical model for predicting permeate flux through a rotating disk taking into consideration concentration dependent diffusivity and viscosity. Experimental data agreed reasonably well with theory although some hysteresis in permeate flux measurements was found. This phenomenon was attributed to solute polymerization in the concentration layer adjacent to the membrane surface. They extended their model to parallel plate systems and considered Blatt's thin channel ultrafiltration data for serum albumin. Their model consistently

underpredicted experimental flux measurements by more than 40%. Misinterpretation of Blatt, et al.'s experimental system together with the limitations of their data, as mentioned earlier, may have been responsible for the apparent disagreement.

Mitra and Lundblad (1978) published data taken in a parallel plate system with immune serum globulin and human serum albumin. They attempted to correlate data using a film theory model in the following form:

$$|\underline{v}_{\underline{w}}| = \underline{A}_1 \langle \underline{u} \rangle^{\underline{B}_1} \ln\left(\frac{\underline{c}_{\underline{w}}}{\underline{c}_{\underline{B}}}\right) \tag{7}$$

where $\underline{A}_1$ and $\underline{B}_1$ are constants. Consistent agreement was found for the value of $\underline{B}_1$, but the value of $\underline{A}_1$ was variable with a 21% standard deviation.

Shen and Probstein (1977) reported a theoretical treatment of the parallel plate system. Their model, like Kozinski and Lightfoot's, considered both concentration-dependent viscosity and diffusivity. Considering the general mass equation, Shen and Probstein utilized a Leveque combination of variables technique. Resulting ordinary differential equations were solved numerically to calculate flux rates. Through comparison of calculated values, they state that the variable fluid property numerical solution can be approximated by a modified film theory. The modification simply amounts to replacing the value of the diffusion coefficient evaluated at $\underline{c}_{\underline{B}}$ by one evaluated at $\underline{c}_{\underline{g}}$.

Shen and Probstein applied their modified film theory model to Blatt's serum albumin data. Data values were extrapolated into the gel-polarized region (extrapolated to limiting values) and were checked by us to be correct. Similar extrapolated values were obtained by Kozinski and Lightfoot. However, Kozinski and Lightfoot, as well as Shen and Probstein appear to use a value for the bulk velocity ($\langle \underline{u} \rangle$)

which, in actuality, is the recirculation rate. Realistic values should be 25% of the recirculation rate.

Originally, Shen and Probstein's calculated flux rates shown in Table 1 of their report agree extraordinarily well with experimental rates. This gives the impression that the modified film theory is accurate. By using the correct values of $\langle \underline{u} \rangle$, the percent error slips from approximately 11% to 30%. This is not good agreement by any means. An interesting fact to note is that the corrected film theory predictions are consistently lower than actual flux rates.

In summary, it appears that the widely used film theory model may not represent an accurate method for the calculation of limiting flux rates in the gel-polarized region. Flux predictions from film theory must be compared with a more exact theory. This information will then be used in the interpretation of existing data of Shen and Probstein.

THEORETICAL DEVELOPMENT

The general mass balance equation of

$$\underline{u} \frac{\partial \underline{c}}{\partial \underline{x}} + \underline{v} \frac{\partial \underline{c}}{\partial \underline{y}} = \frac{\partial}{\partial \underline{y}} \left[\underline{D} \frac{\partial \underline{c}}{\partial \underline{y}} \right] \tag{8}$$

may be transformed to an ordinary differential equation by a method described by Shen and Probstein (1977). This method is analogous to the Leveque solution for laminar flow with constant heat flux at the wall. Assuming constant fluid viscosity, the following mathematical development pertains to a parallel plate system where $\underline{x}$ is measured longitudinally along the membrane surface and $\underline{y}$ is measured transverse to the membrane surface. Consistent with a thin mass transfer boundary layer as compared to the channel half width ($\underline{Sc} > 500$), a linear axial velocity may also be assumed. The respective velocity components are written as

$$\underline{u} = \text{axial velocity} = \frac{3\langle \underline{u} \rangle}{\underline{h}} \underline{y} \tag{9a}$$

$$\underline{v} = \text{transverse velocity} = - |\underline{v}_{\underline{w}}| \tag{9b}$$

where $|\underline{v}_{\underline{w}}|$ is the limiting permeate flux at the membrane surface. Boundary conditions are identical to those previously mentioned for the film theory model applied to the gel-polarized region with the exception that $\underline{y}$ is taken to infinity as the upper limit, namely

$$\underline{y} \to \infty, \ \underline{c} = \underline{c}_{\underline{B}} \tag{10}$$

Transforming the mass balance equation into dimensionless variables using the following relationships

$$\eta = \underline{y}\left(\frac{3\underline{x}\ \underline{D}_{\underline{B}}}{\underline{a}}\right)^{-1/3} \tag{11a}$$

$$\underline{F}(\eta) = \frac{\underline{c}}{\underline{c}_{\underline{B}}} \tag{11b}$$

$$\underline{u} = \left(\frac{3\underline{x}\ \underline{D}_{\underline{B}}}{\underline{a}^2}\right)^{1/3} \eta \tag{12a}$$

$$|\underline{v}_{\underline{w}}| = \left(\frac{\underline{D}_{\underline{B}}{}^2 \underline{a}}{3\underline{x}}\right)^{1/3} \underline{V}_{\underline{w}} \tag{12b}$$

$$\underline{\bar{D}}(\underline{F}) = \frac{\underline{D}(\underline{c})}{\underline{D}(\underline{c}_{\underline{B}})} \tag{12c}$$

where $\underline{a} = 3\langle \underline{u} \rangle / \underline{h}$, and $\underline{V}_{\underline{w}}$ = positive permeate constant. The resulting equation may be expressed

$$\frac{\underline{d}}{\underline{d\eta}}\left[\underline{\bar{D}}\ \frac{\underline{dF}}{\underline{d\eta}}\right] + (\eta^2 + \underline{V}_{\underline{w}})\ \frac{\underline{dF}}{\underline{d\eta}} = 0 \tag{13}$$

where the transformed boundary conditions are

$$\text{at} \quad \eta=0, \; \underline{F} = \underline{F}_g, \; - \underline{V}_w \underline{F}_g = \frac{d\underline{F}}{d\eta}\Big|_{\eta=0} \tag{14a}$$

and,

$$\text{at} \quad \eta=\infty, \; \underline{F} = 1 \tag{14b}$$

Upon integration of the dimensionless solute balance equation with the appropriate boundary conditions the following equation results

$$\frac{1}{\underline{F}_g} = 1 - \underline{V}_w \int_o^\infty \frac{1}{\underline{D}} \cdot \exp\left(- \int_o^\eta \left[\frac{\eta^2 + \underline{V}_w}{\underline{D}} \right] d\eta \right) d\eta \tag{15}$$

If one makes the simplification of constant diffusion coefficient, Equation (15) becomes

$$\frac{1}{\underline{F}_g} = 1 - \underline{V}_w \int_o^\infty \exp\left(-\frac{1}{3}\eta^3\right) \cdot \exp(-\underline{V}_w \eta) d\eta \tag{16}$$

Equation (15) is identical to the relationship derived by Shen and Probstein (1977). Equation (15) may be approximated by an infinite series solution for small values of $\underline{V}_w$. The series solution may be expressed in terms of the gamma function

$$\frac{1}{\underline{F}_g} = 1 - \sum_{\underline{n}=1}^{\infty} (-1)^{\underline{n}+1} \left(\frac{\underline{b}^{\underline{n}/3}}{\underline{n}!} \right) \Gamma\left(\frac{\underline{n}+3}{\underline{n}} \right) \tag{17}$$

where $\underline{b} = 3 \, \underline{V}_w^{\,3}$

The first 6 terms of Equation (17) are:

$$1/\underline{F}_g = 1 - 1.288 \, \underline{V}_w + 0.939 \, \underline{V}_w^{\,2} - 0.499 \, \underline{V}_w^{\,3} + 0.215 \, \underline{V}_w^{\,4} - 0.078 \, \underline{V}_w^{\,5} + 0.025 \, \underline{V}_w^{\,6} \tag{18}$$

For large values of $\underline{V}_w$, Equation (15) may be approximated by carrying out appropriate integration by parts:

$$1/\underline{F}_g = 2/\underline{V}_w^{\,3} - 40/\underline{V}_w^{\,6} + 2.24 \times 10^3/\underline{V}_w^{\,9} - 2.46 \times 10^5/\underline{V}_w^{\,12} + 3.85 \times 10^7/\underline{V}_w^{\,15} \tag{19}$$

For Equations (15) through (19), values of $\underline{V}_w$ are typically within the range of 0 to 10 with $\underline{V}_w$ varying directly with $\underline{F}_g$. A graphical comparison of the approximate equations with regard to the numerical solution of Equation (16) are shown in Fig. 1 and 2. Equations (18) and (19) are plotted under the titles approximation (1) and integration by parts, respectively. As shown in Fig. 1 and 2, Equation (18) is reasonable for $\underline{F}_g$ less than 4 while Equation (19) is accurate for $\underline{F}_g$ greater than about 70.

In lieu of the limited applicability of the approximate solutions, an integral method was applied to the mass balance equation

$$\frac{3\langle \underline{u} \rangle}{\underline{h}} \underline{y} \frac{\partial \underline{c}}{\partial \underline{x}} - |\underline{v}_w| \frac{\partial \underline{c}}{\partial \underline{y}} = \frac{\partial}{\partial \underline{y}}\left[\underline{D} \frac{\partial \underline{c}}{\partial \underline{y}}\right] \tag{20}$$

where the boundary conditions are

$$\text{at} \quad \underline{y}=\delta(\underline{x}), \underline{c} = \underline{c}_B \quad \left.\frac{\partial \underline{c}}{\partial \underline{y}}\right|_{\underline{y}=\delta} = 0 \tag{21a}$$

and

$$\text{at} \quad \underline{y} = 0, \underline{c} = \underline{c}_g, -|\underline{v}_w|\underline{c}_g = \underline{D}_g \left.\frac{\partial \underline{c}}{\partial \underline{y}}\right|_{\underline{y}=0} \tag{21b}$$

Integrating Equation (20) with respect to $\underline{y}$ from $\underline{y} = 0$ to $\underline{y} = \delta$ yields:

$$\frac{3\langle \underline{u} \rangle}{\underline{h}} \left[\frac{\underline{d}}{\underline{dx}} \int_0^{\delta} \underline{y}\underline{c}\underline{dy} - \underline{c}_B \delta \frac{\underline{d}\delta}{\underline{dx}}\right] = |\underline{v}_w| \underline{c}_B \tag{22}$$

Following Doshi, et al. (1971), a concentration profile of the form

$$\underline{c} = \underline{c}_B + (\underline{c}_g - \underline{c}_B)\left(1 - \frac{\underline{y}}{\delta}\right)^{\underline{n}} \tag{23}$$

was assumed. In order for the boundary condition of Equation (21b) to be satisfied,

$$\frac{\underline{n}}{\delta} (\underline{c}_g - \underline{c}_B) \underline{D}_g = |\underline{v}_w| \underline{c}_g \tag{24a}$$

therefore,

$$\delta = \frac{n\underline{D}_g}{|\underline{v}_w|}\left(\frac{\underline{c}_g - \underline{c}_B}{\underline{c}_g}\right), \quad \text{or,} \tag{24b}$$

$$|\underline{v}_w| = \frac{n\underline{D}_g}{\delta}\left(\frac{\underline{c}_g - \underline{c}_B}{\underline{c}_g}\right)$$

Substituting the assumed concentration profile into Equation (22) and completing the integration yields

$$\frac{3\langle\underline{u}\rangle}{\underline{h}(\underline{n}+1)(\underline{n}+2)}\ \frac{d}{d\underline{x}}\ (\delta^2(\underline{c}_g - \underline{c}_B)) = |\underline{v}_w|\underline{c}_B \tag{25}$$

Using Equation (24b) to eliminate $|\underline{v}_w|$ and rearranging gives

$$\frac{d}{d\underline{x}}\ (\delta^3) = \frac{\underline{n}(\underline{n}+1)(\underline{n}+2)\ \underline{D}_g\underline{h}\ \underline{c}_B}{2\langle\underline{u}\rangle\ \underline{c}_g} \tag{26}$$

Integrating Equation (26), noting that at $\underline{x}=0$, $\delta=0$, gives

$$\delta^3 = \frac{\underline{n}(\underline{n}+1)(\underline{n}+2)\ \underline{D}_g\underline{h}\ \underline{c}_B\ \underline{x}}{2\langle\underline{u}\rangle\ \underline{c}_g} \tag{27a}$$

or,

$$|\underline{v}_w| = \underline{n}\ \underline{D}_g\left(\frac{\underline{c}_g - \underline{c}_B}{\underline{c}_g}\right)\left[\frac{2\langle\underline{u}\rangle\ \underline{c}_g}{\underline{n}(\underline{n}+1)(\underline{n}+2)\ \underline{D}_g\underline{h}\ \underline{c}_B\ \underline{x}}\right]^{1/3} \tag{27b}$$

Transforming to dimensionless variables, using Equations (11b, 12b, and 12c) one obtains

$$\underline{V}_w = \frac{\underline{F}_g - 1}{\underline{F}_g}\left[\frac{2\underline{n}^2\ \underline{F}_g}{(\underline{n}+1)(\underline{n}+2)}\right]^{1/3}(\underline{\bar{D}}_g)^{2/3} \tag{28a}$$

or

$$\underline{V}_w = \frac{\underline{F}_g - 1}{\underline{F}_g}\left[\underline{K}\ \underline{F}_g\right]^{1/3}(\underline{\bar{D}}_g)^{2/3} \tag{28b}$$

where $\underline{K} = \dfrac{2\underline{n}^2}{(\underline{n}+1)(\underline{n}+2)}$.

The value of n still remains to be determined. A comparison of numerically calculated values of V_w vs. F_g to those calculated from the integral method for various values of n are shown in Tables 1 and 2 for $\bar{D}_g = 1$.

It bears mentioning at this point that Probstein, Shen, and Leung (1978), in a recent report apply an integral method to the general mass balance equation. Their resulting equation for limiting wall flux is expressed as:

$$|v_w| = \left[\frac{2}{3}\frac{\langle u\rangle D_g^2}{hx}\right]^{1/3} \frac{F_g - 1}{F_g^{2/3}} \tag{29a}$$

or, expressed in terms of V_w

$$V_w = \frac{2}{3}^{1/3}\left[\frac{F_g - 1}{F_g^{2/3}}\right] \bar{D}_g^{2/3} = \left[\frac{2}{3} F_g\right]^{1/3}\left[\frac{F_g - 1}{F_g}\right] \bar{D}_g^{2/3} \tag{29b}$$

It is apparent that their limiting flux equation is identical to Equation (28b) for the case $n = 2$, $K = 2/3$.

In this analysis it was assumed that constant n was some function of F_g. The integral method was applied again to ascertain the form of this function.

Multiplying Equation (20) throughout by y

$$\frac{3\langle u\rangle}{h} y^2 \frac{\partial c}{\partial x} - |v_w|\, y \frac{\partial c}{\partial y} = y \frac{\partial}{\partial y}\left(D \frac{\partial c}{\partial y}\right) \tag{30}$$

and integrating with respect to y from $y = 0$ to $y = \delta$ yields:

$$\frac{3\langle u\rangle}{h}\left[\frac{d}{dx}\left(\int_0^\delta y^2\, c\, dy\right) - \delta^2 c_B \frac{d\delta}{dx}\right] + |v_w| \int_0^\delta c\, dy = |v_w|\, \delta c_B - \int_0^\delta D \frac{\partial c}{\partial y}\, dy \tag{31}$$

Substituting the concentration profile of Equation (23) and assuming linear concentration dependency of diffusion coefficient, gives:

$$\frac{3\langle u\rangle}{h}\left[\frac{2(c_g - c_B)}{(n+1)(n+2)(n+3)}\right]\frac{d}{dx}(\delta^3) + \frac{|v_w|\,\delta(c_g - c_B)}{n+1} = D_g c_g - D_B c_B + \frac{1}{2}\left(-\frac{dD}{dc}\right)(c_g^2 - c_B^2) \quad (32)$$

Combining Equation (32) with Equations (24b) and (26), one gets

$$\frac{3nc_B}{(n+3)c_g} + \frac{n}{n+1}\left[1 - \frac{c_B}{c_g}\right] = B \quad (33)$$

where

$$B = \frac{\bar{D}_g F_g - 1}{\bar{D}_g (F_g - 1)} + \frac{A}{2}\,\frac{F_g + 1}{F_g} \quad \text{and} \quad A = \frac{c_g}{\bar{D}_g}\left(-\frac{dD}{dc}\right) \quad (33a)$$

Converting to dimensionless variables and rearranging Equation (33)

$$F_g = \frac{2n^2}{(n+3)}\,[B(n+1) - n] \quad (34)$$

For values of $B < 1 + 2/F_g$, Equation (34) may be converted to a more usable form:

$$n = \frac{(4B-3)F_g + [(3-2B)^2 F_g^2 + 24\,BF_g]^{1/2}}{2[2 + (1-B)\,F_g]} \quad (35a)$$

For values of $B \geq 1 + 2/F_g$, it is assumed that $n = \infty$, $K = 2$.

For the case of constant diffusion coefficient, $\bar{D}_g = 1$, $A = 0$, and $B = 1$, Equation (35a) simplifies to:

$$n = (1/4)\,[F_g + (F_g^2 + 24\,F_g)^{1/2}] \quad (35b)$$

Comparison of the integral method with variable n and constant diffusion coefficient is made with the numerical solution of Equation (16) in Table 3. Agreement between calculated values is excellent with less than 1% error.

Use of the variable n integral solution in calculating flux rates is favored over the more tedious approximate solutions to Equation (16) from the standpoint of accuracy and wide-range of application.

Numerical solutions of the film theory model [Equation (3) for constant wall concentration and constant wall flux] along with the exact solution model are plotted in Fig. 3. All solutions are for constant fluid properties. The range of $\underline{V}_{\underline{w}}$ values is from 0 to 7. This range is believed to encompass most probable operating conditions. Results indicate that the film theory model agrees with the exact solution for $\underline{F}_{\underline{g}} < 4$ when the constant wall concentration boundary condition is used. It is also shown that for higher values of $\underline{F}_{\underline{g}}$, the exact solution model consistently predicts higher permeate flux rates than do either of the film theory models.

Even though in the gel-polarized region where the CWC boundary condition seems reasonable, the CWF boundary condition gives better agreement, up to $\underline{F}_{\underline{g}} \simeq 12$. It is not clear why the CWF boundary condition gives better agreement than the CWC boundary condition, which has been widely used. One may note that in the case of pre-gel polarized model, which is somewhat analogous to the corresponding reverse osmosis system, Gill, et al. (1965, 1971) have shown that the CWF boundary condition is more realistic.

The effect of concentration dependent diffusion coefficient is shown in Fig. 4. For the case of bovine serum albumin at pH 7.4, the parameter $\underline{A}$ can be estimated to be:

$$\underline{A} = \frac{\underline{c}_{\underline{g}}}{\underline{D}_{\underline{g}}} \left(-\frac{d\underline{D}}{d\underline{c}} \right) = 0.187$$

where

$$\underline{D}(\underline{c}) = (5.9 - 0.016\underline{c}) \times 10^{-7} \quad \text{[from Probstein (1978b)]}$$

APPLICATION OF THEORY TO EXPERIMENTAL DATA

The availability of reliable data in the area of macromolecular ultrafiltration is rather limited. A characteristic problem encountered when comparing

experimental flux rates with theory is the lack of a reliable value of the solute "gel" concentration and the concentration dependent diffusion coefficient. Several diffusional studies of bovine serum albumin have been reported by Keller, et al. (1971), Phillies, et al. (1976), and Doherty and Benedek (1974). Unfortunately, results are often contradictory. It appears that the degree of the functional dependence of the diffusion coefficient upon solute concentration is strongly dependent upon solution pH.

If one accepts the functional form of the film theory model, it is possible to extrapolate the value of $\underline{c}_g$ from ultrafiltration experiments. By measuring limiting flux rates at several values of $\underline{c}_B$, the results are plotted semilogarithmically and a straight line is drawn through the data points. This line is extended to the point of zero flux where the corresponding value of $\underline{c}_B$ is taken to equal $\underline{c}_g$.

In light of the developed integral solution, the potential error is apparent. By using experimental flux rates at low values of $\underline{c}_B$, which is common in the literature, it is possible that an erroneous prediction of $\underline{c}_g$ will result. This process is depicted in Fig. 5. This line of reasoning may be a possible explanation of the fact that Porter (1972), using the film theory method of analysis, calculated a change in the value of $\underline{c}_g$ from 45 g/100 cc to 28 g/100 cc for human serum albumin by simply varying the channel height of his test unit.

Since the integral solution may be approximated by the film theory model at values of $\underline{F}_g < 4$, it is feasible to use the semilogarithmic, straight line extrapolation of experimental flux rates at high values of $\underline{c}_B$ in cases where $\underline{c}_g$ is approximately known. Whenever possible, it is recommended that an independent method be used in the determination of $\underline{c}_g$ as done by Kozinski and Lightfoot (1972).

The data of Probstein, et al. (1978a) were analyzed in terms of the constant diffusion coefficient integral method solution. Numerical calculations of flux rates using modified film theory were also included for purposes of comparison. For the experiments involving bovine serum albumin at a pH of 7.4, we adopt their value of $\underline{c}_{\underline{g}}$ = 58.0 g/100 cc which is widely accepted. Instead of using their value of $\underline{D}_{\underline{g}} = 6.7 \times 10^{-7}$ cm^2/sec, we chose $\underline{D}_{\underline{g}} = 4.8 \times 10^{-7}$ cm^2/sec. For the experiments involving bovine serum albumin at a pH of 4.7, we chose $\underline{D}_{\underline{g}} = 3.35 \times 10^{-7}$ cm^2/sec and $\underline{c}_{\underline{g}}$ = 58.0 g/100 cc as opposed to their values of $\underline{D}_{\underline{g}} = 5.6 \times 10^{-7}$ cm^2/sec and $\underline{c}_{\underline{g}}$ = 34.0 g/100 cc. Calculations are shown in Tables 4 and 5. Critical dimensions of the test unit are: length(l) = 48.0 cm, width(w) = 7.62 cm, and half-height(h) equals approximately 0.19 cm.

Modified Film Theory [Probstein, et al. (1978a)]

$$|\underline{v}_{\underline{w}}| = 1.31\, \underline{D}_{\underline{g}}^{2/3} \left[\frac{\underline{D}_{\underline{B}}^2 \langle \underline{u} \rangle}{\underline{h}\underline{l}}\right]^{1/3} \ln \frac{\underline{c}_{\underline{g}}}{\underline{c}_{\underline{B}}}$$

Integral Method Solution

$$|\underline{v}_{\underline{w}}| = 1.5 \left(\frac{\underline{D}_{\underline{B}}^2 \langle \underline{u} \rangle}{\underline{h}\underline{l}}\right)^{1/3} \left[\frac{\underline{c}_{\underline{g}}/\underline{c}_{\underline{B}} - 1}{\underline{c}_{\underline{g}}/\underline{c}_{\underline{B}}}\right] \left[\underline{K} \frac{\underline{c}_{\underline{g}}}{\underline{c}_{\underline{B}}}\right]^{1/3} (\underline{D}_{\underline{g}}^{2/3})$$

where $\underline{K}$ is defined by Equations (28b) and (35b).

It should be noted that while the selected values of $\underline{D}_{\underline{g}}$ and $\underline{c}_{\underline{g}}$ used in the integral solution calculations are certainly within an expected range of values, it is in no way implied that they are actual values. The calculations set forth in Tables 4 and 5 are intended as an example to show that the integral solution represents a viable method to calculate flux rates within the range of uncertainty of the value of $\underline{D}_{\underline{g}}$. It is possible to revise above calculations by considering concentration dependent diffusion coefficient, that is, using Equation (35a)

instead of (35b) to evaluate $\underline{n}$. Such numerical exercise is differed until more accurate information on $\underline{D}_{\underline{g}}$ and $\underline{c}_{\underline{g}}$ is available. Important point is that the straight line extrapolation of experimental data using film theory could give misleading results.

ACKNOWLEDGMENT

The authors wish to express their gratitude to Professor Ronald F. Probstein of the Massachusetts Institute of Technology and William F. Blatt of the Amicon Corporation for their cooperation during the preparation of this report. The authors are also grateful to the member companies of The Institute of Paper Chemistry for their support of the graduate program.

NOTATION

$\bar{A}$ = membrane pure water permeability constant (cm^3/dyne-s)

a = $3\langle u\rangle/h$ (1/s)

c = solute concentration (g solute/100 cc solution)

D = diffusion coefficient (cm^2/sec)

d = hydraulic diameter of membrane channel (cm)

$\bar{D}$ = $D(c)/D_B$

F = c/c_B

h = channel half-height (cm)

k = mass transfer coefficient (cm/sec)

l = total length of membrane section (cm)

P = total pressure at a point (dynes/cm^2)

Re = Reynolds number = $\langle u\rangle d/\nu$

Sc = Schmidt number = ν/D

u = axial velocity (cm/sec)

$\langle u\rangle$ = average axial velocity (cm/sec)

v = transverse velocity (cm/sec)

$|v_w|$ = limiting permeate velocity at membrane surface (cm/sec)

V_w = positive permeate constant

w = width of flow channel (cm)

x = axial distance coordinate

y = transverse distance coordinate

Greek Letters

$\delta(x)$ = concentration (mass) boundary layer thickness

π = osmotic pressure (dynes/cm^2)

η = similarity variable

Γ = gamma function

$\Delta\pi$ = osmotic pressure difference across membrane (dynes/cm^2)

ΔP = total pressure difference across membrane (dynes/cm^2)

ν = kinematic viscosity

Subscripts

g = at the gelling condition

w = at the membrane wall

B = at the bulk condition

P = at the permeate condition

LITERATURE CITED

Blatt, W. F., Personal communication (1978).

Blatt, W. F., A. Dravid, A. S. Michaels, and L. Nelsen, "Solute Polarization and Cake Formation in Membrane Ultrafiltration: Causes, Consequences, and Control Techniques," in Membrane Science and Technology, J. E. Flinn, ed., p. 47, Plenum Press, New York, N.Y. (1970).

Doherty, P., and G. B. Benedek, "The Effect of Electric Charge on the Diffusion of Macromolecules," J. Chem. Phys. 61, 5426 (1974).

Doshi, M. R., A. K. Dewan, and W. N. Gill, "The Effect of Concentration Dependent Viscosity and Diffusivity on Concentration Polarization in Reverse Osmosis Flow Systems," AIChE Symp. Series, 68, 323 (1971).

Gill, W. N., C. Tien, and D. W. Zeh, "Concentration Polarization Effects in a Reverse Osmosis System," Ind. Eng. Chem. Fundam., 4, 433 (1965).

Gill, W. N., L. J. Derzansky, and M. R. Doshi, "Convection Diffusion in Laminar and Turbulent Hyperfiltration (Reverse Osmosis) Systems," in Surface and Colloid Science, Volume 4, E. Matijevic, ed., p. 261, Wiley-Interscience, New York, N.Y. (1971).

Goldsmith, R. L., "Macromolecular Ultrafiltration with Microporous Membranes," Ind. Eng. Chem. Fundam., 10, 113 (1971).

Keller, K. H., E. R. Canales, and S. I. Yum, "Tracer and Mutual Diffusion Coefficients of Proteins," J. Phys. Chem., 75, 379 (1971).

Kozinski, A. A., and E. N. Lightfoot, "Protein Ultrafiltration: A General Example of Boundary Layer Filtration," AIChE J., 18, 1031 (1972).

Michaels, A. S., "New Separation Technique for CPI," Chem. Eng. Progr., 64, 31 (1968).

Mitra, G., and J. L. Lundblad, "Ultrafiltration of Immune Serum Globulin and Human Serum Albumin: Regression Analysis Studies," Sep. Sci. Tech., 13, 89 (1978).

Phillies, G. D. J., G. B. Benedek, and N. A. Mazer, "Diffusion in Protein Solutions at High Concentrations: A Study by Quasielastic Light Scattering Spectroscopy," J. Chem. Phys., 65, 1883 (1976).

Porter, M. C., "Concentration Polarization with Membrane Ultrafiltration," Ind. Eng. Chem. Prod. Res. Develop., 11, 234 (1972).

Probstein, R. F., J. S. Shen, and W. F. Leung, "Ultrafiltration of Macromolecular solutions at High Polarization in Laminar Channel Flow," Desalination, 24, 1 (1978).

Probstein, R. F., Personal Communication (1978).

Shen, J. J. S., and R. F. Probstein, "On the Prediction of Limiting Flux in Laminar Ultrafiltration of Macromolecular Solutions," Ind. Eng. Chem. Fundam., 16, 459 (1977).

Table 1. Values of Integral Method Constant K for Various Values of n

n	K
1	0.3333
2	0.6667
3	0.9000
4	1.0667
5	1.1905
∞	2.0000

Table 2. Comparison of Numerically Calculated Values of $\underline{V}_{\underline{w}}$ to those Calculated from the Integral Method for Various Values of $\underline{n}$

$\underline{F}_{\underline{g}}$	Integral method $\underline{V}_{\underline{w}}$ ($\underline{n}$=5)	Numerical integration $\underline{V}_{\underline{w}}$	Integral method $\underline{V}_{\underline{w}}$ ($\underline{n}\rightarrow\infty$)
58.0	4.03	4.64	4.79
29.0	3.14	3.53	3.74
19.3	2.70	3.00	3.20
14.5	2.41	2.60	2.86
11.6	2.20	2.32	2.61
9.7	2.03	2.11	2.41
8.3	1.89	1.94	2.24

Table 3. Comparison of Integral Method with Variable n with Numerical Solution of Equation (15)

			Integral method	Numerical integration
F_g	n	K	V_w	V_w
116.0	60.86	1.91	6.00	5.99
58.0	31.74	1.824	4.65	4.64
29.0	17.05	1.691	3.53	3.53
19.3	12.05	1.584	2.96	3.00
14.5	9.53	1.496	2.60	2.60
11.6	7.98	1.421	2.33	2.32
9.7	6.95	1.358	2.12	2.11
8.3	6.17	1.300	1.94	1.94
2.32	2.53	0.803	0.700	0.694

Table 4. Experimental Flux Rates with BSA at pH = 7.4 — Probstein, et al. (1978), Probstein (1978)

Bulk concentration c_B (g/100 cc)	Average velocity (cm/s)	h (cm)	Experimental flux (cm/s) × 10^4	Predicted flux × 10^4 Modified film theory* (cm/s)	Predicted flux × 10^4 Integral method** (cm/s)	K
1.87	5.75	0.190	3.00	2.95	2.87	1.71
1.80	11.51	0.190	3.67	3.76	3.67	1.72
1.78	17.26	0.190	4.17	4.32	4.22	1.72
1.76	23.01	0.190	4.67	4.77	4.66	1.72

*$D_g = 6.7 \times 10^{-7}$ cm^2/sec

c_g = 58.0 g/100 cc

**$D_g = 4.8 \times 10^{-7}$ cm^2/sec

c_g = 58.0 g/100 cc

Table 5. Experimental Flux Rates with BSA at pH = 4.7 — Probstein (1978)

Bulk concentration c_B (g/100 cc)	Average velocity (cm/s)	h (cm)	Experimental flux (cm/s) × 10^4	Predicted flux × 10^4 Modified film theory* (cm/s)	Predicted flux × 10^4 Integral method** (cm/s)	K
2.44	12.15	0.180	2.63	2.63	2.63	1.64
2.57	18.22	0.180	2.92	2.95	2.94	1.62
2.74	24.29	0.180	3.15	3.16	3.15	1.61
3.88	10.93	0.200	2.02	2.02	2.00	1.51
4.23	16.40	0.200	2.20	2.22	2.19	1.48
4.42	16.40	0.200	2.18	2.17	2.14	1.46
4.42	21.87	0.200	2.33	2.39	2.35	1.46
3.11	5.85	0.187	1.83	1.85	1.83	1.57
3.16	9.35	0.187	2.13	2.14	2.12	1.56

*$D_g = 5.6 \times 10^{-7}$ cm^2/sec

c_g = 34.0 g/100 cc

**$D_g = 3.35 \times 10^{-7}$ cm^2/sec

c_g = 48.0 g/100 cc

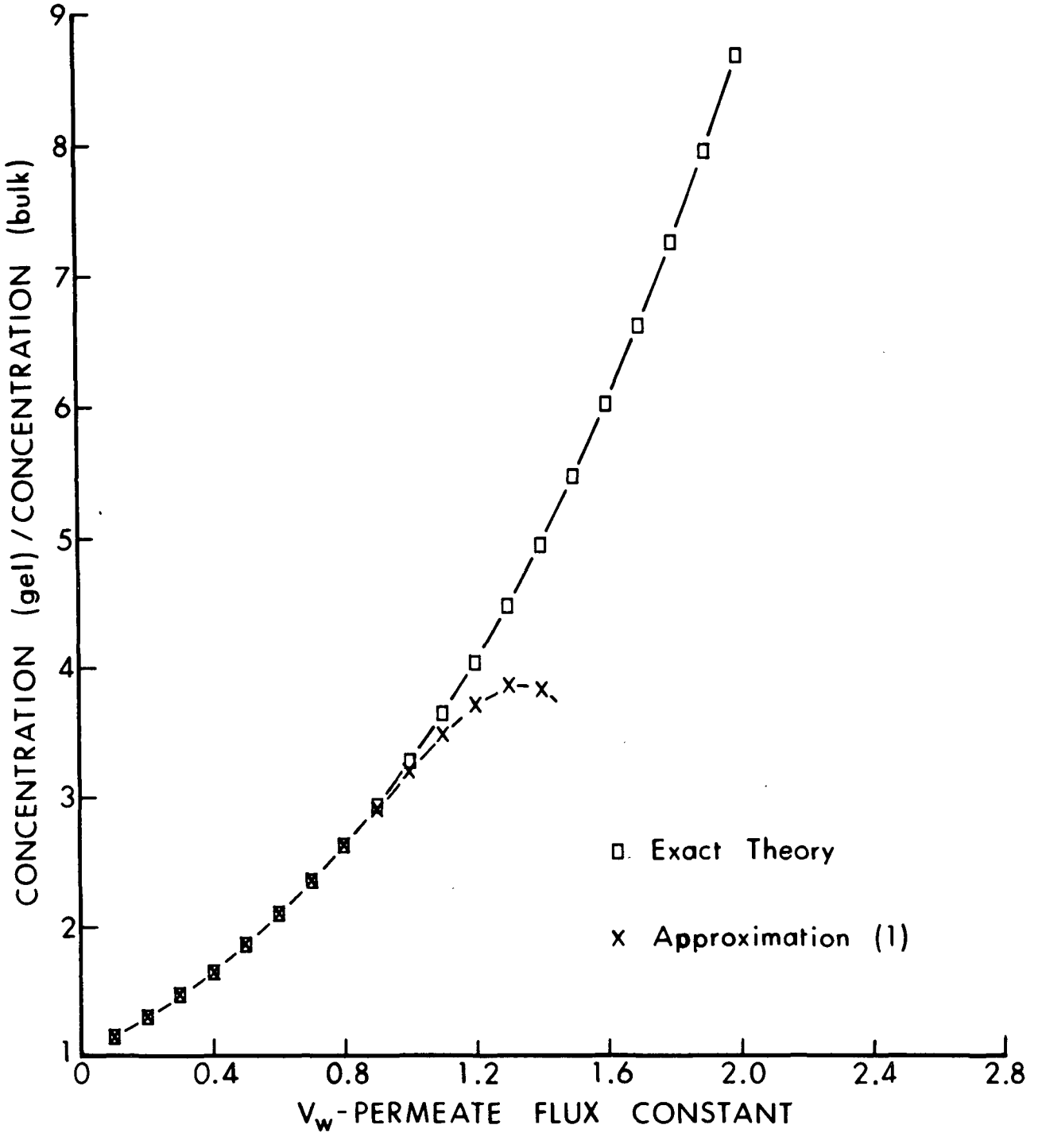

Fig. 1. Comparison of exact UF equation to approximate solutions.

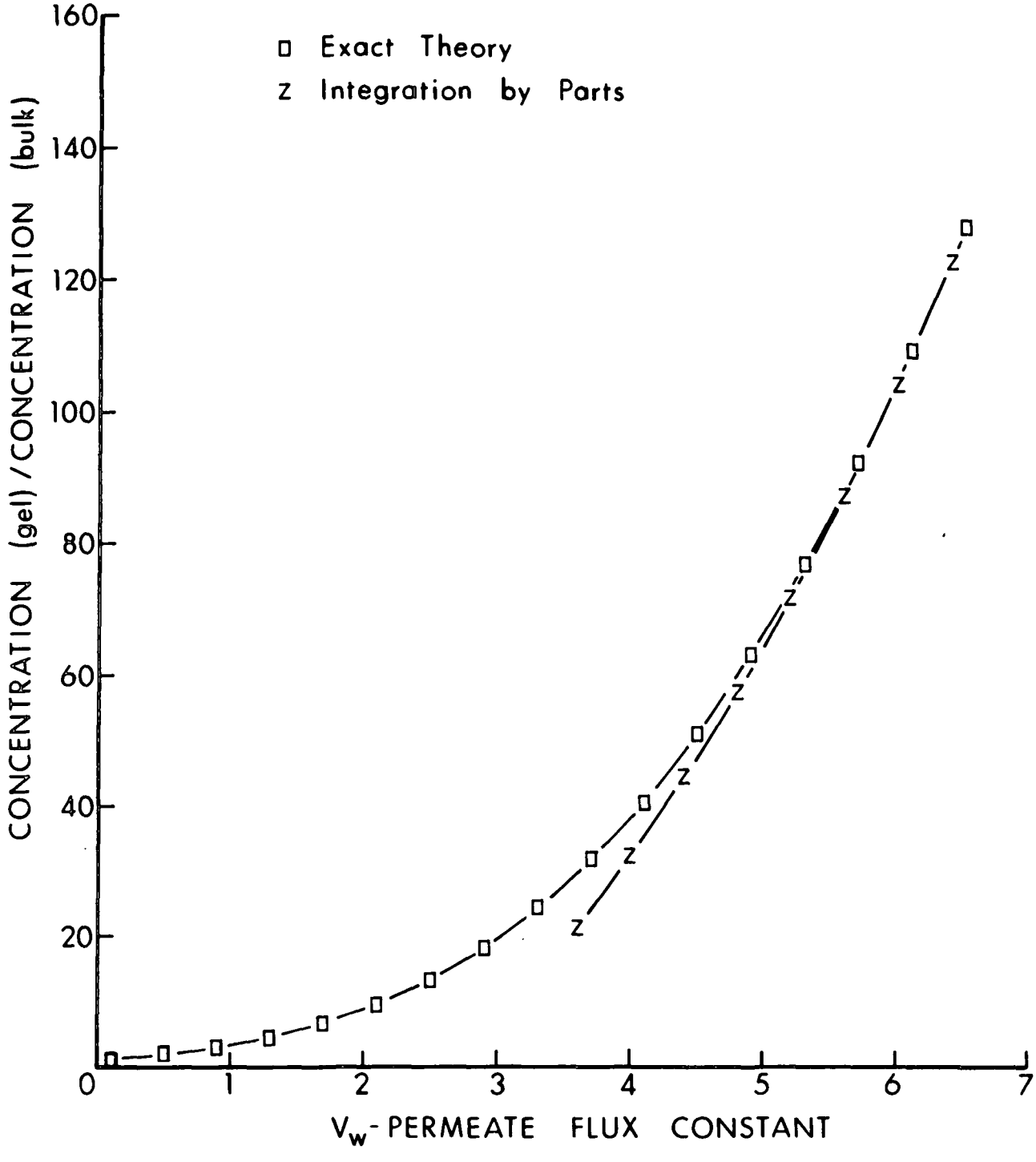

Fig. 2. Comparison of exact UF equation to approximate solutions.

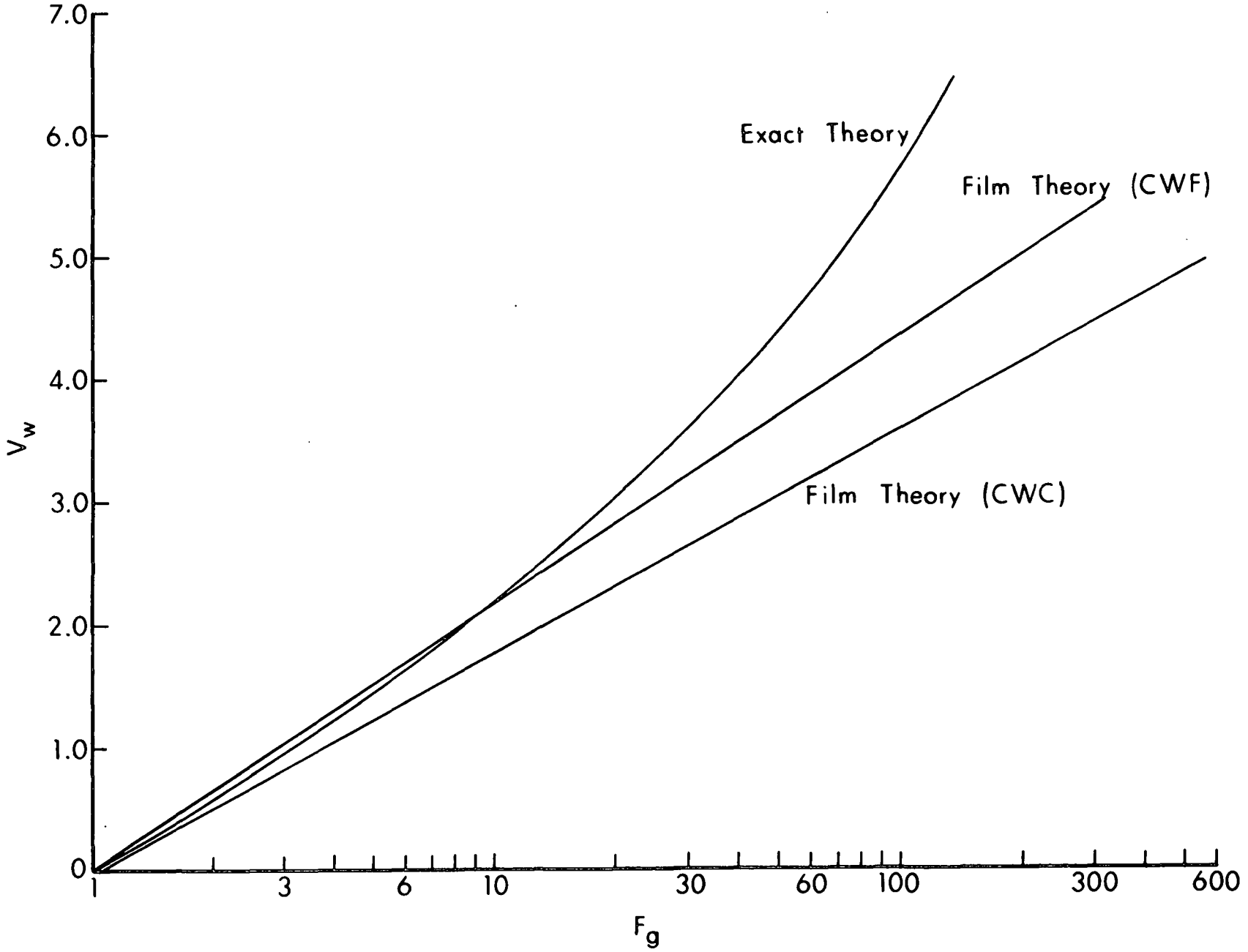

Fig. 3. Comparison of integral method solution with film theory models.

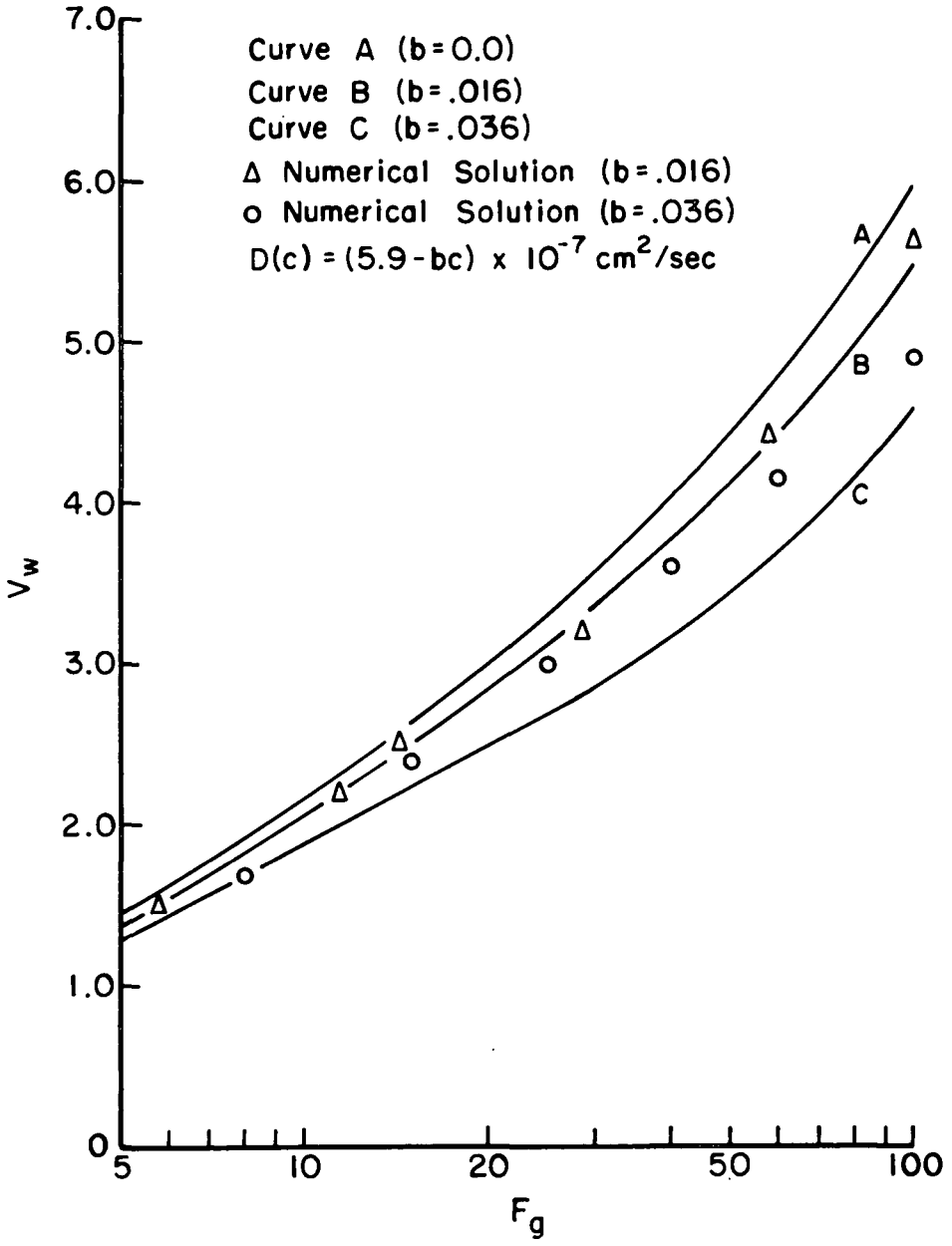

Fig. 4. Effect of increasing diffusional concentration dependence upon integral method predictions.

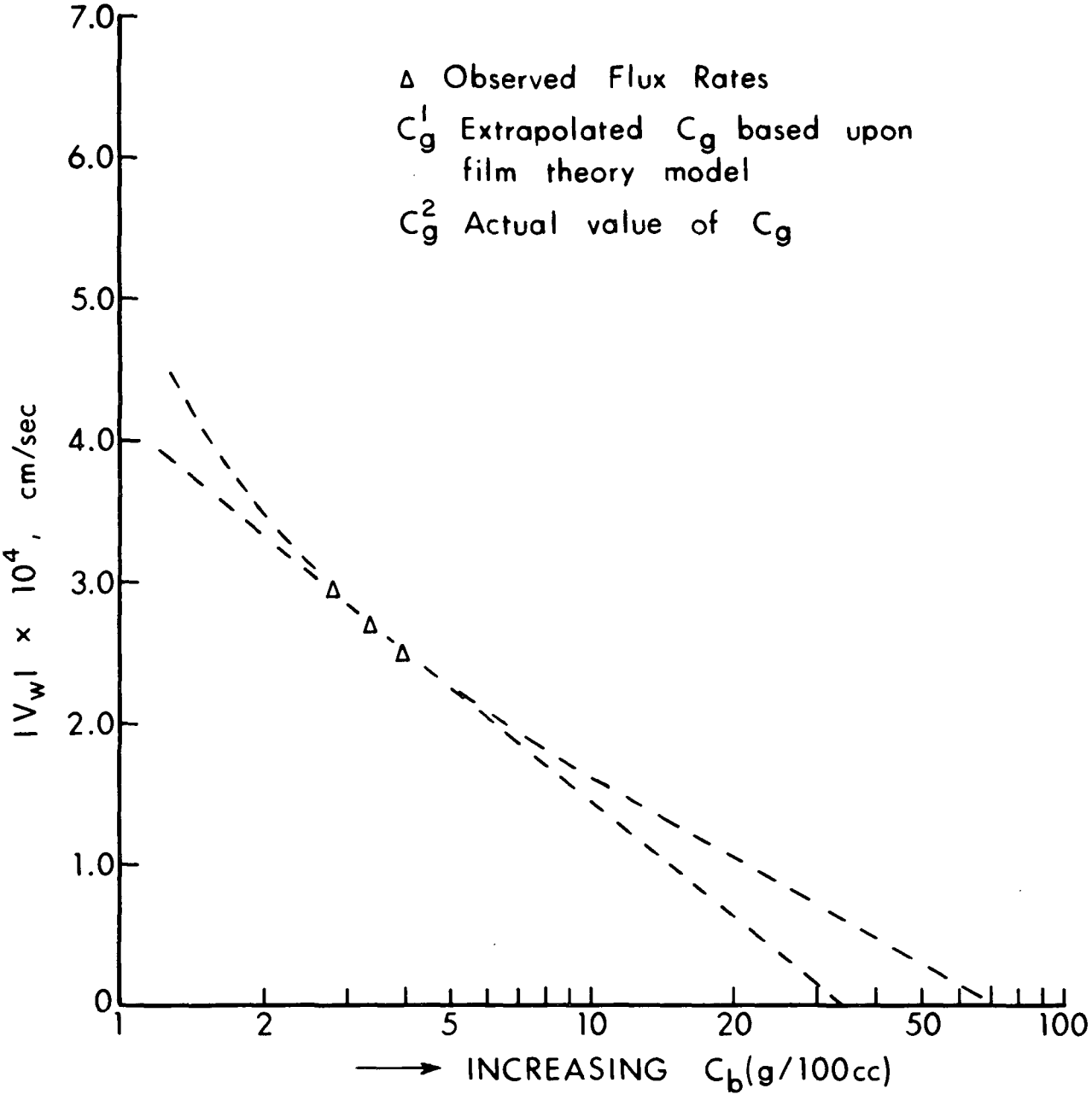

Fig. 5. Film theory method for determining the value of c_g.